Bonding in the Si_2H_2 Isomers: A Topographical Study

D. B. Chesnut

P. M. Gross Chemical Laboratory, Duke University, Durham, North Carolina 27708

Received 22 May 2001

ABSTRACT: *Chemical bonding in the isomers of the formally triply bonded Si_2H_2 system are studied from the point of view of electron localization function (ELF) bond basin populations and atoms-in-molecules (AIM) delocalization indices. Calculation carried out at the B3LYP/6-31 + G(d,p) and MP2 (FC)/6-31 + G(d,p) level leads to ELF topographies and basin populations that are in good agreement with our intuitive chemical pictures of bonding in these molecules. One single, two double, and one triple silicon–silicon bonds are found in the four isomers. It is shown that, with one AIM exception, ratios of basin populations and delocalization indices are consistent and useful in characterizing the nature of the chemical bonding involved.* © 2002 John Wiley & Sons, Inc. Heteroatom Chem 13:53–62, 2002; DOI 10.1002/hc.1106
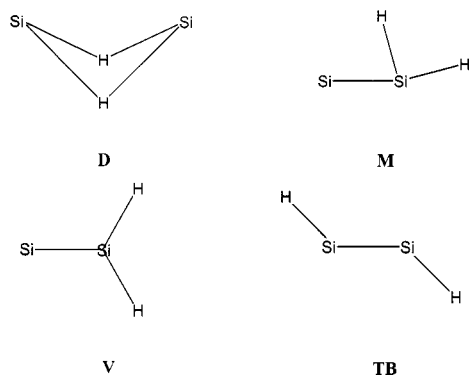
INTRODUCTION

Although for many years multiple bonds between elements beyond the first long row were considered unstable (the "double bond rule"), recent review articles [1–6] show that much progress has been made in the synthesis and characterization of these species. Much interesting theoretical work has appeared [7–14] including specific studies of compounds containing silicon [7,10,14], germanium [8,13], and gallium [12,13]. Grützmacher and Fässler [14] have presented the first topographical analysis of these systems to which we later refer.

Correspondence to: D. B. Chesnut; e-mail: dbc@chem.duke.edu.

A great deal of the fascination with these multiply bonded species involving elements such as Si, Ge, and Ga and others is the departure from "classical" multiple bonded geometries, i.e., for doubly bound carbon, one realizes a planar geometry about the double bond and linearity for triply bound species, whereas such is not the case for elements of the second long row and higher where bent (and bridged) structures are the rule rather than the exception. These unusual structures are understood in terms of the proclivity of the fragments containing the heavier elements to form low-spin states upon breaking of the heavy atom bond, in contrast to the corresponding elements of the first row that prefer high-spin states. Carter and Goddard [15] correlated the bond energy with the singlet-triplet energy of the bond-broken fragments, work that was extended by Trinquier and Malrieu [16] that enabled predictions regarding geometry; this combined work is generally referred to as the CGMT model.

In this paper we focus on the bonding in the four low-energy isomers of Si_2H_2, perhaps the simplest compounds exhibiting the unusual bonding characteristics of the multiply bound higher atomic number species, and, for purposes of comparison, their C_2H_2 analogs. Si_2H_2 has been fully characterized by Grev and Schaefer [10] at a high level of theory (CCSD(T) with a tz2df basis) following up the earlier calculations of Lischka and Köhler [7]. Si_2H_2 has four stable isomers all, within 20 kcal/mol of each other in order of increasing energy: the dibridged (**D**, C_{2v}) or butterfly, monobridged (**M**, C_s), disilavinylidene (**V**, C_{2v}), and the trans-bent (**TB**, C_{2h}) species shown in Scheme 1.

SCHEME 1

For the bonding analysis we employ two approaches that have emerged in recent years, which show great promise of fulfilling our desire to better pin down the still elusive nature of chemical bonding. These are the delocalization index of Fradera, Austen, and Bader [17] based on the atoms-in-molecules (AIM) approach [18], and bond basin populations from the electron localization function (ELF) approach of Becke and Edgecombe [19] as extensively developed by Savin and Silvi and coworkers [20–27]. Using these two methods we set out to characterize the nature of the bonds in the Si_2H_2 and C_2H_2 species as related to their singly and doubly bound counterparts. Examination of the structures seen in Scheme 1 would suggest a variety of bonding situations, as, indeed, we find.

THEORETICAL BACKGROUND

The Electron Localization Function

ELF is a robust descriptor of chemical bonding based on topological analyses of local quantum mechanical functions related to the Pauli exclusion principle. The local maxima of the function define localization attractors corresponding to core, bonding (located between the core attractors of different atoms), and nonbonding electron pairs and their spatial arrangement. It is of special interest to chemists in that the resulting isosurfaces of ELF density tend to conform to the classical Lewis picture of bonding.

Becke and Edgecombe [19] pointed out that the conditional pair probability for same spin electrons has the form

$$P_{\text{cond}}^{\sigma\sigma}(\vec{r}, s) = \frac{1}{3}\left[\sum_j^{\sigma} |\nabla\varphi_j|^2 - \frac{1}{4}\frac{|\nabla\rho_\sigma|^2}{\rho_\sigma} \right]s^2 + \cdots \quad (1)$$

for an electron at point $\vec{r}$ and another a distance s away (averaged over a spherical shell of radius s). The coefficient of the quadratic term is the local Pauli

kinetic energy density, the excess kinetic energy electrons have (because of the Pauli exclusion principle) compared to a bosonic system of the same density [22]. When it is small the Fermi hole at $\vec{r}$ is large and one would expect to find pairs of electrons of *opposite* spin in the region; when it is large, the converse is true.

For a closed shell single determinantal wavefunction built from Hartree–Fock or Kohn–Sham orbitals, φ_j, the ELF function of position $\vec{r}$ is *defined* as

$$\eta = \frac{1}{1 + (D/D_h)^2} \quad (2)$$

where

$$D = \frac{1}{2}\sum_{j=1}^{N} |\nabla\varphi_j|^2 - \frac{1}{8}\frac{|\nabla\rho|^2}{\rho}$$

$$D_h = \frac{3}{10}(3\pi^2)^{2/3}\rho^{5/3}$$

$$\rho = \sum_{j=1}^{N} |\varphi_j|^2 \quad (3)$$

and where the scaling factor was chosen to be the homogeneous electron gas kinetic energy density of a system of the same electron density. The ELF function can be viewed as a local measure of the Pauli repulsion between electrons because of the exclusion principle and allows one to define regions of space that are associated with different electron pairs in a molecule or solid. The position where ELF attains a maximum value (the attractor) can be used as an electron pair's signature [25].

Using the vector field of the gradient of the electron localization function, the topology of the ELF function can be used to define basins within which one or more electron pairs are to be found [21–23,26]. These subsystems are defined in terms of zero flux surfaces; the gradient paths end at what are called *attractors* within each subsystem. The region of 3-D space traversed by all gradient paths that terminate at a given attractor defines the *basin* of the attractor. ELF basins are labeled as either core or valence basins. Core basins contain a nucleus while valence basins do not; hydrogen basins are taken as exceptions since, although they contain a proton, they represent a shared pair interaction. A valence basin is characterized by its number of connections to core basins, referred to as its synaptic order. Basins are connected if they are bounded by part of a common surface. A simple covalent bond basin would be connected to two core basins and be of synaptic order two; a lone pair basin would be monosynaptic. More complex bonding basins can be polysynaptic.

The population of a basin Ω_i, N_i, is given by integrating the total electron density, $\rho(\vec{r})$, over the basin volume. These populations are particularly important in

$$N_i = \int\limits_{\Omega_i} \rho(\vec{r})\, d\vec{r} \qquad (4)$$

that they tend to reflect delocalization effects and, in the case of bond basins, the bond order.

The Delocalization Index

Bader's AIM approach [18] is based on the electron density, $\rho(\vec{r})$, a key observable in a molecules, description. The gradient field of the electron density is used to define atomic basins, which can be integrated over to obtain AIM atomic basin electron populations. The delocalization index is defined in terms of the electron pair density as it relates to the AIM atomic basins.

The electron pair density [28,29], $P_2(\vec{r}_1, \vec{r}_2)$, is the diagonal part of the reduced second-order density matrix and is normalized as

$$\int d\vec{r}_1 \int d\vec{r}_2 P_2(\vec{r}_1, \vec{r}_2) = \int d\vec{r}_1 (N-1)\rho(\vec{r}_1) = N(N-1)$$

$$(5)$$

where $\rho(\vec{r}_1)$ is the electron number density and N the total number of electrons. It proves convenient to define the pair density in terms of a quantity explicitly referencing the antisymmetric character of electron wavefunctions,

$$P_2(\vec{r}_1, \vec{r}_2) = \rho(\vec{r}_1)\rho(\vec{r}_2)[1 + f(\vec{r}_1, \vec{r}_2)] \qquad (6)$$

so that

$$\frac{P_2(\vec{r}_1, \vec{r}_2)}{\rho(\vec{r}_2)} - \rho(\vec{r}_1) = \rho(\vec{r}_1) f(\vec{r}_1, \vec{r}_2) \qquad (7)$$

The quantity on the left is the *conditional probability* of finding an electron at $\vec{r}_1$ given that there is one at $\vec{r}_2$, minus the number density at $\vec{r}_1$, $\rho(\vec{r}_1)$, where integration over the coordinates of *all* other electrons has taken place. This quantity (either side of Eq. (7)) is the *Fermi hole* [28,29] associated with the reference electron at $\vec{r}_2$.

If we integrate the pair density over two AIM basins, Ω_i and Ω_j, we obtain by definition the quantity N_{ij}, the interbasin pair number, and, using Eq. (6) can write [18,30,31]

$$N_{ij} = \int\limits_{\Omega_i} d\vec{r}_1 \int\limits_{\Omega_j} d\vec{r}_2 P_2(\vec{r}_1, \vec{r}_2)$$

$$= \int\limits_{\Omega_i} d\vec{r}_1 \int\limits_{\Omega_j} d\vec{r}_2 \rho(\vec{r}_1)\rho(\vec{r}_2)[1 + f(\vec{r}_1, \vec{r}_2)]$$

$$= N_i N_j + \int\limits_{\Omega_i} d\vec{r}_1 \int\limits_{\Omega_j} d\vec{r}_2 \rho(\vec{r}_1)\rho(\vec{r}_2) f(\vec{r}_1, \vec{r}_2)$$

$$= N_i N_j - F_{ij} \qquad (8)$$

where N_i and N_j are the basin electron numbers and where here, in contrast to Fredera et al. [17], we have explicitly introduced the negative sign in the definition of F_{ij} because it is generally positive. Because of the relations in Eqs. (5) and (6) the following sum rule for F_{ij} obtains:

$$\sum_j N_{ij} = N_i(N-1) = N_i N - \sum_j F_{ij}$$

$$\sum_j F_{ij} = N_i \qquad (9)$$

The diagonal elements of F_{ij} are also important since it can be shown that they are intimately related to the variance, s_i^2, of the electron number in a basin [30,31] by

$$s_i^2 = N_{ii} - N_i(N_i - 1) = N_i - F_{ii} \qquad (10)$$

These relations have also been clearly presented by Savin, Noury, and coworkers [22,26].

It is the sum of the off-diagonal terms $F_{ij} + F_{ji} = 2F_{ij} \equiv \delta_{ij}$ in the AIM approach that Fradera, Austen, and Bader [17] refer to as the *delocalization index* and use as a quantitative measure of the sharing of electrons between basins Ω_i and Ω_j; they also denote F_{ii} as the *atomic localization index*.
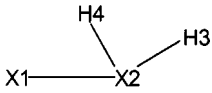
Details of the Calculations

The AIM and ELF calculations were carried out employing the TopMod Package of Noury and coworkers [32] in the B3LYP approach [33,34] with a 6-31+G(d,p) basis. Step sizes of 0.1 au and box sizes that extended 5.0 au from the outermost atomic coordinates in each direction were typically used. The TopMod package sacrifices some accuracy for efficiency and, according to the authors [32], is thought to be accurate to a few percent, sufficient for comparative studies. Optimizations and energies (including unscaled zero-point energies) were carried out at the MP2(FC)/6-31 + G(d,p) level with Gaussian 98 [35]; all the geometries were confirmed to be equilibrium structures.

RESULTS AND DISCUSSION

Geometries

The geometries used in this study were obtained at the MP2(FC)/6-31 + G(d,p) level and are given in Table 1 along with the relative energies (including

TABLE 1 Structural Parameters for the Silicon and Carbon Systems (Å and degrees) Optimized at the MP2(FC)/6-31 + G(d,p) Level[a]

Molecule	r_{XX}	r_{XH}	a_{HXH}	a_{HXX}	Other	E
Silicon compounds						
H_3SiSiH_3	2.340	1.476	108.7	110.2		
H_2SiSiH_2	2.169	1.472	112.9	118.6	29.9[b]	
Si_2H_2						
D	2.208 (2.208)	1.657 (1.684)	72.4	48.2	104.8[c] (103.2)	0.0
M	2.125 (2.119)	1.480[d] (1.474)	106.1 (105.0)	158.0[e] (157.5)		8.8
		1.625[f] (1.629)		51.9[g] (52.5)		
		1.702[h]				
V	2.210	1.475	113.5	123.3		11.6
TB	2.108	1.480		124.4		16.2
Carbon compounds						
H_3CCH_3	1.525	1.090	107.7	111.2		
H_2CCH_2	1.339	1.081	117.9	121.5		
C_2H_2						
linear	1.221	1.064		180.0		0.0
M	1.275	1.071[d]	122.4	186.9[e]		46.5
		1.202[f]		64.5[g]		
		1.323[h]				
V	1.308	1.085	120.0	120.0		47.7
D	1.307	1.265	82.8	58.8		78.8

[a]Relative energies including zero-point energies (*E*, kcal/mol) at this same level are also indicated. Experimental data are given in parentheses for the **D** and **M** structures from Ref. [36] and [37], respectively.
[b]Dihedral angle of butterfly structure.
[c]Fold angle of butterfly structure.
[d]X2–H3 distance.
[e]H3–X2–(H4)–X1 angle.
[f]X2–H4 distance.
[g]H4–X2–X1 angle.
[h]X1–H4 distance.

unscaled zero-point energies) at the same level of theory. Structural data for the singly and doubly bound systems are also given; although Si_2H_4, just as Si_2H_2, has a variety of stable isomers [9], the low energy trans-bent structure for Si_2H_4 is used here to represent the doubly bound case for silicon. The geometries of the silicon compounds agree well with those of Grev and Schaefer [10] as might be expected since a split valence with polarization basis generally does well at the MP2 level. The optimized geometries also agree well with the known structures of the **D** [36] and the **M** [37] forms obtained from microwave studies. It is a bit surprising that our relative energies are so close to those of Grev and Schaefer since they used a large basis at an advanced level of theory (CCSD(T)), but sometimes this happens when energy *differences* are being considered. As has been noted before, it is remarkable to have so many isomers so close in energy.

So far as we know, the equilibrium geometries of the high energy carbon isomers are new. Because we were interested in comparing the corresponding silicon and carbon cases we did not search the entire C_2H_2 energy surface but rather optimized the carbon cases starting at the geometries of the silicon compounds with suitably reduced bond distances. As one might have expected, linear acetylene is by far the most stable, the other carbon isomers being rather high in energy.

One can note from Table 1 that bond distances for bridging hydrogens are longer than for the non-bridging types, a result consistent with the structure of diborane, for example, and to be understood in their description as two-electron, three-center bonds.

Bonding Analysis

Fredera, Austen, and Bader [17] point out that molecular formation reduces the number of pairs between two atoms (N_{ij} is reduced as F_{ij} increases, Eq. (8)) while increasing the pair formation within

each (AIM) atomic basin. They take the reduction in N_{ij} to be the result of the formation of shared pairs between atoms and is the basis for their contention that $F_{ij} + F_{ji} = 2F_{ij} \equiv \delta_{ij}$, the delocalization index, provides a quantitative measure of the sharing of electrons between atoms. They are, however, quick to point out that the delocalization index is not identified with a bond order because, with the exception of equally shared pairs (no bond polarization), it does not determine the number of contributing Lewis electron pairs. They illustrate this with the delocalization indices from Hartree-Fock calculations on N$_2$, NO$^+$, CN$^-$, and CO of 3.042, 2.405, 2.210, and 1.574, respectively, for this isoelectronic sequence with increasing bond polarization. Our premise is that, if polarization effects are kept relatively constant, the *ratios* of delocalization indices should provide insight into the nature of the bonds involved.

In a like manner, although the ELF bond basins population, N_i, can be taken as a measure of a topological bond order [22] (more properly 0.5N_i), when atoms of differing electronegativity are involved or lone pairs are nearby, this simple picture becomes more complex [38–40]. Again, however, we contend that, if the local molecular situation is reasonably constant, ratios of bond basin populations can yield useful information concerning the bonding.

We believe that this *consistency of local molecular structure* is reasonably present in the Si$_2$H$_2$ and C$_2$H$_2$ systems studied here. Tables 2 and 3 provide the unmodified data for the bond basin populations and corresponding AIM delocalization indices and, key to our further discussion, ratios of these quantities relative to the corresponding doubly bound species, chosen arbitrarily as reference.

Before proceeding to our results we present in Scheme 2 two bonding pictures that will be used in the discussion. Chemists like to picture bonding in terms of orbitals, and, while this is usually useful and often predictive, these are *pictures* which, in our case, are *after the fact*. In the left-hand column the structures are given in terms of tetrahedral-like hybrids headed at the top by the classical case of acetylene. The **D** and **M** structures are pictured as involving two-electron, three-center hydrogen bridging bonds, while the **V** structure involves tetrahedral orbitals on one center and sp^2 + (empty)p on the other. In the right-hand column the structures are pictured in terms of the preferred doublet state fragments coming together to form the various molecules. The trans bent (**TB**) structure is, of course, the classic case for that structure involving dative-like bonds from the fragment lone pairs plus a p—π bond, while Grev and Schaefer [10] picture the bridged **D** and **M** structures in ways where the hydrogen atoms

TABLE 2   Bond Basin Populations (N_i) and Delocalization Indices (δ_{ij}) for the Heavy Atom Bonds in the Disilicon and Dicarbon Compounds[a]

Molecule	N_i	$N_{i, rel}$	δ_{ij}	$\delta_{ij, rel}$
Silicon compounds				
H$_3$SiSiH$_3$	1.946	0.516	0.722	0.488
H$_2$SiSiH$_2$	3.772	1.0	1.480[b]	1.0
Si$_2$H$_2$				
D	1.793	0.475	1.070	0.723
M	3.206 (2)	0.850	1.512	1.022
V	3.100 (2)	0.822	1.608	1.086
TB	5.830	1.546	2.084[b]	1.408
Carbon compounds				
H$_3$CCH$_3$	1.775	0.516	0.954	0.505
H$_2$CCH$_2$	3.440 (2)	1.0	1.890	1.0
C$_2$H$_2$				
linear	5.205	1.513	2.846	1.506
M	3.541 (2)	1.029	2.222	1.176
V	3.290 (2)	0.956	2.082	1.102
D	2.144	0.623	1.956	1.035

[a] $N_{i,rel}$ and $\delta_{ij, rel}$ represent values relative to those for the corresponding doubly bonded species. A "2" in parentheses in the N_i column indicates that the population given is the total of two bonding basins in the bond region. The X$_2$H$_2$ species are listed in increasing relative energy.
[b] A non-nuclear attractor (NNA) is found in the Si—Si bond midpoint in this molecule. An "effective" Si—Si delocalization index is determined by presuming that half of the NNA belongs to each silicon atom. This removes the NNA from the picture while preserving the sum of the F_{ii} and F_{ij} terms.

interact with a previously empty p orbital. We note in passing that the fragment pictures in these cases do not properly reflect the location of the lone pairs as indicated by the ELF topography. There is no analogous fragment-like structure for acetylene since the fragments in that case prefer a high spin configuration, nor can the **V** molecule be represented in terms of the SiH fragments in their doublet configuration. Similarly, the **TB** case cannot be represented even partially with tetrahedral-like orbitals. As we shall see, the ELF results provide support for the tetrahedral hybrids pictures for the **D, M**, and **V** structures and are not in agreement with the doublet fragment pictures for the **D** and **M** molecules. The ELF results for **TB** are consistent with the doublet fragments picture given in Scheme 2. The AIM delocalization index provides no support for either set of picture since it represents an interaction between basins localized on singular atoms and has no representation of the bonding region as such.

The ELF isosurfaces ($\eta = 0.82$) are given in Fig. 1 for the four Si$_2$H$_2$ isomers; the surfaces for the C$_2$H$_2$ species (not given) are similar. The resemblance of the **D, M**, and **V** isosurfaces to the tetrahedral representations in Scheme 2 is apparent; the **TB** case is

TABLE 3 Bond Basin Populations (N_i), and the Delocalization Indices (δ_{ij}), for the Heavy-Atom-to-Hydrogen Bonds in the Disilicon and Dicarbon Compounds[a]

H4

H3

X1———X2

Molecule	N_i	$N_{i,\ rel}$	δ_{ij}	$\delta_{ij,\ rel}$
Silicon compounds				
H_3SiSiH_3	1.981	0.986	0.619	0.905
H_2SiSiH_2	2.010	1.0	0.684	1.0
Si_2H_2				
D	1.863	0.927	0.580	0.848
M	1.974[b]	0.982[b]	0.790[c]	1.135[c]
	1.876[d]	0.933[d]	0.708[e]	1.035[e]
			0.576[f]	0.842[f]
V	1.996	0.983	0.722	1.129
TB	2.000	0.995	0.782	1.143
Carbon compounds				
H_3CCH_3	2.000	0.960	0.958	0.988
H_2CCH_2	2.084	1.0	0.970	1.0
C_2H_2				
linear	2.286	1.097	0.938	0.967
M	2.128[b]	1.021[b]	0.944[c]	0.973[c]
	1.558[d]	0.748[d]	0.676[e]	0.697[e]
			0.382[f]	0.394[f]
V	1.985	0.952	0.914	0.942
D	1.434	0.688	0.514	0.530

[a] $N_{i,rel}$ and $\delta_{ij,rel}$ represent values relative to those for the corresponding doubly bonded species. The X_2H_2 species are listed in increasing relative energy.
[b] H_3.
[c] X2–H3 bond region.
[d] H4.
[e] X2–H4 bond region.
[f] X1–H4 bond region.

unique and will be dealt with separately. Visually or by direct output from the ELF code one can locate the attractors corresponding to the various basins. In all cases attractors are located where atoms are seen (hydrogen and core basins) and at those locations where orbital vertices meet or where lone pairs are indicated. Thus, as has been realized for some time now, the electron localization function approach provides additional quantitative substance to the valence shell electron pair repulsion (VSEPR) ideas [41–44]. In the **D** and **M** cases the location of the lone pair attractors is very slightly off the Si–Si line, 6 degrees in the first case and 3 degrees in the second. The two attractors in the **M** case, indicative of a Si–Si (bent) double bond, are closer to the hydrogen-bearing silicon (1.24 Å) than to the silicon holding the lone pair (2.13 Å).

The populations of the basins illustrated in Fig. 1 (and contained in Tables 2 and 3) are consistent with the above qualitative bonding notions. Hydrogen and core basin populations are close to what one
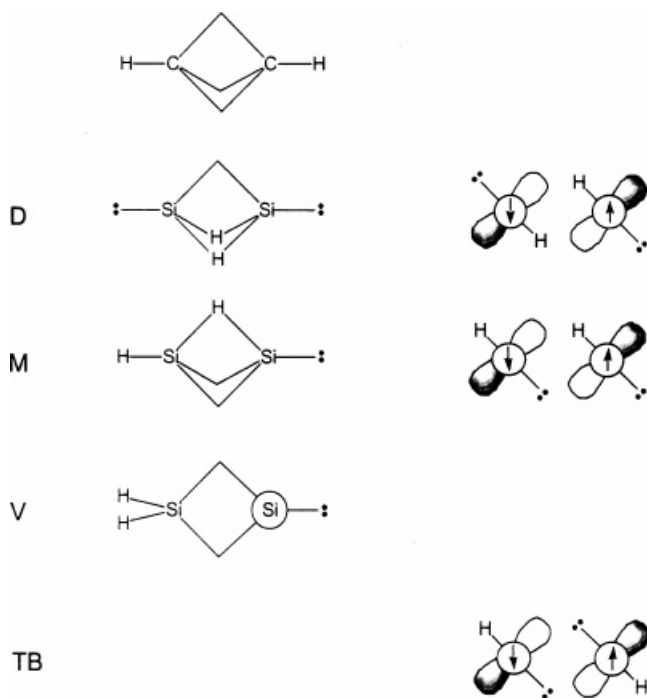
SCHEME 2

would expect (2 and 10 for hydrogen and silicon, respectively) and are mentioned no further. Here we concentrate on the lone pair and bonding basins. Those for the **D** butterfly structure (a) clearly show lone pair basins ($N_i = 2.16$) behind each silicon and a bent single silicon—silicon bond basin with a population of $N_i = 1.79$, both populations being in the range expected for a pair of electrons. The monobridged structure **M** (b) shows a pair of basins linking the silicon atoms (with a total population of 3.21 electrons), clearly what we have come to regard as the signature of a double bond (although not all double bonds possess two attractors); as mentioned before, these two basins are much closer to the hydrogen bearing silicon atom and in this instance, because of the presence of the bridging hydrogen bond, represent a kind of bent double bond. The silicon lone pair basin contains 2.78 electrons. The disilavinylidene structure **V** (c) clearly exhibits a pair of basin corresponding to a double bond ($N_{ii} = 3.10$ for the sum of the two basins) and a silicon lone pair basin with 2.74 electrons. Finally, the trans bent **TB** structure (d) shows what Grützmacher and Fässler [14] have called a "slipped" multiple bond extending from the bottom of one silicon to the top of the other through the silicon—silicon bonding region. The total electron population for the basins contributing to this region is 5.83 and one would regard this as a triple bond, indeed the only silicon—silicon triple bond found in
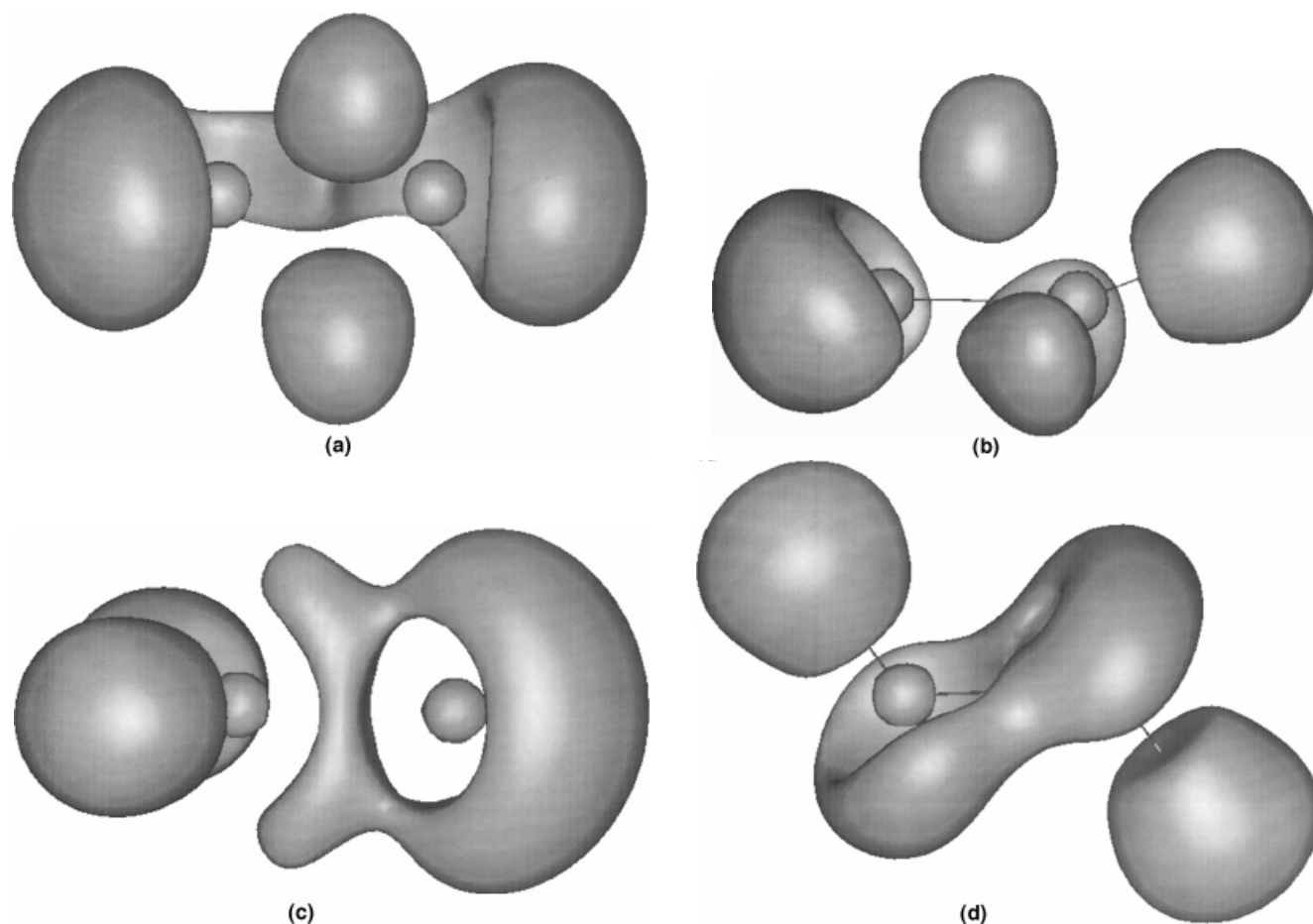
FIGURE 1   ELF isosurfaces ($\eta = 0.82$) for the (a) **D**, (b) **M**, (c) **V**, and (d) **TB** Si$_2$H$_2$ isomers. The **D** isomer displays lone pairs to the left and right of the silicon core basins; proton basins are in the front with the bent single silicon–silicon bond to the rear. The monobridged (**M**) surfaces shows a silicon lone pair basin to the left with two bond basins representing the (bent) double bond closer to the silicon atom on the right. The disilavinylidene (**V**) isosurfaces clearly exhibit lone pair and double bond basins, while the trans bent (**TB**) isomer shows the torus-shaped slipped triple bond between silicon atoms.

our analysis of the Si$_2$H$_2$ isomers. The shape of the overall bond basins found for **TB** is similar to what Grützmacher and Fässler found in their ELF study of trans bent Si$_2$H$_4$ where a slipped double bond is present.

The basin structure for trans bent Si$_2$H$_2$ is of special interest and provides additional insight to the bonding involved. Figure 2 shows to proper scale the location of all the attractors in this system, from a side-on view in (a) to a top view in part (b). The two views show that the non-hydrogen bonding basins in this case actually correspond to six attractors, two located in the midpoint region between silicon atoms ($N_i = 1.44$ for the two basins), and two basins (with populations each of 2.19) on each silicon essentially above the nucleus and on the sides opposite those of the bound hydrogens. As indicated before, the total population of 5.83 from the six basins clearly suggests a triple bond.

The structure of the attractors in the **TB** case suggests further interpretation. Some time ago we presented a study of the amide bond [45] in systems such as formamide whose resonance forms are illustrated in Scheme 3. The ELF isosurfaces found in such amide-bond-containing molecules clearly showed basin structure in the vicinity where one would expect the nitrogen lone pair to reside; we suggested this represented a signature of the amide bond. In a like manner, the structure of the attractors found for trans bent Si$_2$H$_2$ suggests a similar signature and interpretation. That is, as was done for digallyne by Grützmacher and Fässler [14], we can also write here resonance structures for trans bent Si$_2$H$_2$ as shown in Scheme 4 consistent with the ELF topography shown by this triply bonded molecule. We suggest this resonance mixture (of unknown composition, just as in the amide case) contributes to the isosurface structure seen and may be taken as the signature of the
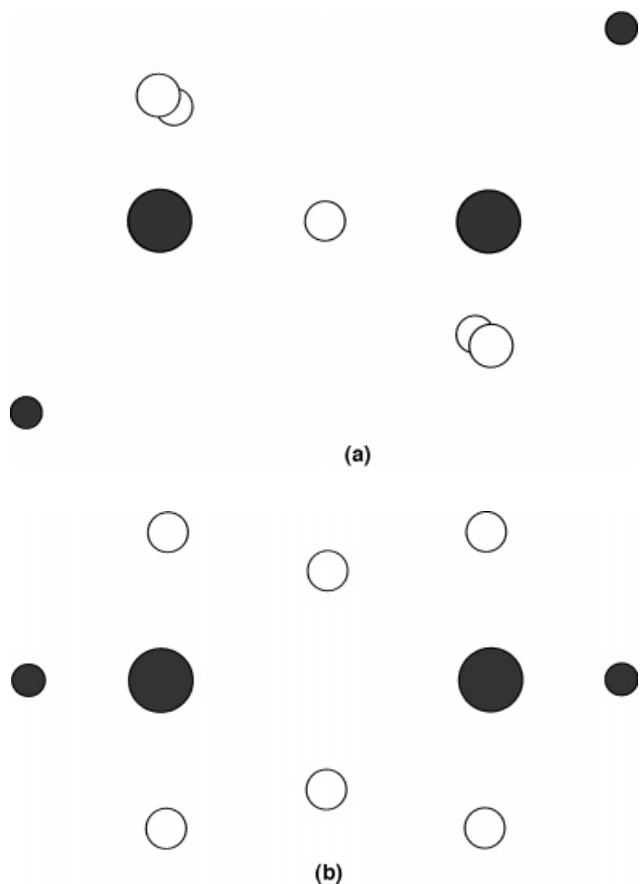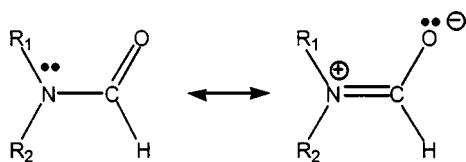
SCHEME 4

FIGURE 2 Two scale views of the ELF attractors for the trans bent (**TB**) isomer seen (a) side on and (b) from above the molecule (linear in projection). Bond basins are represented as open circles while core and hydrogen basins are filled. The side view (a) exhibits the central two attractors (of the six total in the bonding region) as superimposed; the top view (b) shows them to be closer together than the attractors near the silicon atoms that we have associated with lone pair character.
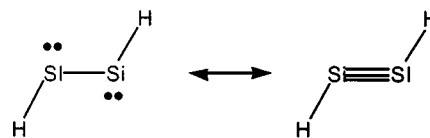
slipped triple bond in trans bent Si_2H_2. The lone pair character of multiple bonds for the heavier elements has been discussed by Power [3,4].

Parameter Ratios and Bond Orders

Any topological division of an electronic system will be sensitive to the approach used to define the scalar

SCHEME 3

field whose gradient field then defines basins and basin attractors. The AIM approach in which atomic basins are derived from the scalar field of the electron density is a very natural one, but, while atomic basin properties seem natural in this regard, the electron pair density divided up into interbasin contributions is not as transparent. ELF basins are defined quantities although based on strong physical arguments regarding the Fermi hole and the corresponding tendency of electron pairs to occupy different regions of space. It is, indeed, striking that ELF basin populations correspond as closely as they do to our chemical expectations of electron pairing. As we have mentioned earlier, complications to our simplistic expectations arise in both approaches when lone pairs are nearby or when bonds are polarized [38–40].

We indicated earlier that, while the bonding parameters (both ELF bond basin populations and AIM delocalization indices) may not in an absolute sense reflect our simple ideas of bond orders, we believe that ratios of these parameters referenced to a suitable standard may be a more viable measure of the bonding situation. Table 2 shows that while the ELF bond populations for ethane, ethene, and ethyne are less than 2, 4, and 6, the ratios (referenced to the double bond case) very nicely reflect the relative bond orders (0.52, 1.0, and 1.51) we expect on chemical grounds. For these same cases the delocalization indices are once again in the expected 1:2:3 ratio, being 0.50, 1.0, and 1.51. Accepting this premise then, we examine the orders of the silicon–silicon and carbon–carbon bonds in the various isomers.

The ELF results for both Si_2H_2 and C_2H_2 cases are consistent with our pictures given in Scheme 2: the silicon–silicon bond in **D** is single, in **M** and **V** essentially double, and in the **TB** case (the linear molecule for carbon) triple. In all cases the inclusion of the bridging hydrogen bonds brings the total bonding "between" silicon (and carbon) to three. The delocalization index ratios also yield similar results with the exception of the **D** cases (both silicon and carbon isomers), which indicate more nearly a double rather than a single bond. Because the ELF results so clearly match up with our simple orbital picture (our orbital prejudices!), we consider them more appropriate and think the results for the

delocalization index for the **D** cases is somehow flawed in our interpretation.

The hydrogen bonding parameters are included for completeness in Table 3. Here our parameter ratio interpretation divides the results into two classes of molecules depending on whether silicon or carbon is involved. For the silicon isomers all the hydrogen bonds, bridging or not, are essentially equivalent and equal to a unit bond order. The spread in values for the delocalization index is somewhat larger but the same conclusion obtains. For the carbon cases, however, the bonds divide themselves into what we would call the "normal" situations and the bridging cases. While the normal hydrogen bonds are essentially of unit order, those for the bridging cases are noticeably reduced, and, accordingly, must be considered weaker. These results would seem to arise from the fact that the silicon isomers are all reasonable stable species with a spread of energies of only some 20 kcal/mol, while for the carbon molecules all but the highly stable linear cases are very high in energy and relatively unstable.

SUMMARY

Interpretation of the ELF basin topography and basin populations provide a clear picture of the bonds in the four Si$_2$H$_2$ isomers, a picture described well by a simple hybrid orbital description. With the exception of the dibridged **D** case, consideration of the delocalization index provides support for the ELF interpretation. It is not clear why this particular case should be an exception.

ACKNOWLEDGMENTS

REFERENCES

[1] West, R. Angew Chem Int Ed Engl 1987, 26, 1202.
[2] Driess, M.; Grützmacher, H. Angew Chem Int Ed Engl 1996, 33, 828.
[3] Power, P. P. J Chem Soc Dalton 1998, 18, 2939.
[4] Power, P. P. Chem Rev 1999, 99, 3463.
[5] Jutzi, P. Angew Chem Int Ed Engl 2000, 39, 3797.
[6] Cundari, T. R. Chem Rev 2000, 100, 807.
[7] Lischka, H.; Köhler, H.-J. J Am Chem Soc 1983, 105, 6646.
[8] Grev, R. S.; Deleeuw, B. J.; Schaefer III, H. F. Chem Phys Lett 1990, 165, 257.
[9] Trinquier, G. J Am Chem Soc 1996, 112, 2130.
[10] Grev, R. S.; Schaefer III, H. F. J Chem Phys 1992, 97, 7990.
[11] Jacobsen, H.; Ziegler, T. J Am Chem Soc 1994, 116, 3667.
[12] Xie, Y.; Grev, R. S.; Gu, J.; Schaefer III, H. F.; Schleyer, P. v. R.; Su, J.; Li, X.-W.; Robinson, G. H. J Am Chem Soc 1998, 120, 3773.
[13] Allen, T. L.; Fink, W. H.; Power, P. P. J Chem Soc Dalton 2000, 3, 407.
[14] Grützmacher, H.; Fässler, T. F. Chem Eur J 2000, 6, 2317.
[15] Carter, E. A.; Goddard III, W. A. J Phys Chem 1986, 90, 998.
[16] (a) Trinquier, G.; Malrieu, J.-P. J Am Chem Soc 1987, 109, 5303; (b) Malrieu, J.-P.; Trinquier, G. J Am Chem Soc 1989, 111, 5916.
[17] Fradera, X.; Austen, M. A.; Bader, R. F. W. J Phys Chem A 1999, 103, 304.
[18] Bader, R. F. Atoms in Molecules: A Quantum Theory; Oxford University Press: Oxford, 1994.
[19] Becke, A. D.; Edgecombe, K. E. J Chem Phys 1990, 92, 5397.
[20] Savin, A.; Becke, A. D.; Flad, J.; Nesper, R.; Preuss, H.; von Schnering, H. G. Angew Chem Int Ed Engl 1991, 30, 409.
[21] Silvi, B.; Savin, A. Nature 1994, 371, 683.
[22] Savin, A.; Silvi, B.; Colonna, F. Can J Chem 1996, 74, 1088.
[23] Kohout, M.; Savin, A. Int J Quantum Chem 1996, 60, 875.
[24] Savin, A.; Nesper, R.; Wengert, S.; Fässler, T. Angew Chem Int Ed Engl 1997, 36, 1809.
[25] Marx, D.; Savin, A. Angew Chem Int Ed Engl 1997, 36, 2077.
[26] Noury, S.; Colonna, F.; Savin, A.; Silvi, B. J Mol Struct 1998, 450, 59.
[27] Kouhout, M.; Savin, A. J Comput Chem 1997, 18, 1431.
[28] McWeeny, R. Rev Mod Phys 1960, 32, 335.
[29] McWeeny, R. Methods of Molecular Quantum Mechanics, 2nd ed.; Academic Press: New York, 1989.
[30] Bader, R. F. W.; Stephens, M. E. Chem Phys Lett 1974, 26, 445.
[31] Bader, R. F. W.; Stephens, M. E. J Amer Chem Soc 1975, 97, 7391.
[32] Noury, S.; Krokidis, X.; Fuster, F.; Silvi, B. Comput Chem 1999, 23, 597.
[33] Becke, A. D. J Chem Phys 1993, 98, 5648.
[34] Lee, C.; Yang, W.; Paar, R. G. Phys Rev 1988, B 37, 785.
[35] Frisch, M. J.; Trucks, G. W.; Schlegel, H. B.; Scuseria, G. E.; Robb, M. A.; Cheeseman, J. R.; Zakrzewski, V. G.; Montgomery, Jr., J. A.; Stratmann, R. E.; Burant, J. C.; Dapprich, S.; Millam, J. M.; Daniels, A. D.; Kudin, K. N.; Strain, M. C.; Farkas, O.; Tomasi, J.; Barone, V.; Cossi, M.; Cammi, R.; Mennucci, B.; Pomelli, C.; Adamo, C.; Clifford, S.; Ochterski, J.; Petersson, G. A.; Ayala, P. Y.; Cui, Q.; Morokuma, K.; Malick, D. K.; Rabuck, A. D.; Raghavachari, K.; Foresman, J. B.; Cioslowski, J.; Ortiz, J. V.; Baboul, A. G.; Stefanov, B. B.; Liu, G.; Liashenko, A.; Piskorz, P.; Komaromi, I.; Gomperts, R.; Martin, R. L.; Fox, D. J.; Keith, T.; Al-Laham, M. A.; Peng, C. Y.; Nanayakkara, A.; Gonzalez, C.; Challacombe, M.; Gill, P. M. W.;

Johnson, B.; Chen, W.; Wong, M. W.; Andres, J. L.; Gonzalez, C.; Head-Gordon, M.; Replogle, E. S.; Pople, J. A. Gaussian 98, Revision A.7; Gaussian, Inc., Pittsburgh PA, 1998.

[36] Bogey, M.; Bolvin, H.; Demuynck, C.; Destombes, J.-L. Phys Rev Lett 1991, 66, 413.

[37] Cordonnier, M.; Bogey, M.; Demuynck, C.; Destombes, J.-L. J Chem Phys 1992, 97, 7984.

[38] Fourré, I.; Silvi, B.; Chaquin, P.; Sevin, A. J Comput Chem 1999, 20, 847.

[39] Llusar, R.; Beltrán, A.; Andrés, J.; Noury, S.; Silvi, B. J Comput Chem 1999, 20, 1517.

[40] Chesnut, D. B. Heteroatom Chem 2000, 11, 341.

[41] Gillespie, R. J.; Nyholm, R. S. Q Rev 1957, 11, 334.

[42] Gillespie, R. J. Molecular Geometry; Van Nostrand Reinhold: London, 1972.

[43] Gillespie, R. J.; Hargittai, I. VSEPR Model of Molecular Geometry; Allyn and Bacon: Boston, 1991.

[44] Gillespie, R. J.; Robinson, E. A. Angew Chem 1996, 108, 539; Angew Chem Int Ed Engl 1996, 35, 495.

[45] Chesnut, D. B. J Phys Chem A 2000, 104, 7635.